Int J Appl Earth Obs Geoinformation 84 (2020) 101956

Contents lists available at ScienceDirect

Int J Appl Earth Obs Geoinformation

journal homepage: www.elsevier.com/locate/jag

Update and spatial extension of strategic forest inventories using time series remote sensing and modeling

Chen Shang[a,*], Nicholas C. Coops[a], Michael A. Wulder[b], Joanne C. White[b], Txomin Hermosilla[b]

[a] Integrated Remote Sensing Studio, Department of Forest Resources Management, Faculty of Forestry, University of British Columbia, 2424 Main Mall, Vancouver, British Columbia, V6T 1Z4, Canada

[b] Canadian Forest Service (Pacific Forestry Centre), Natural Resources Canada, 506 West Burnside Road, Victoria, British Columbia, V8Z 1M5, Canada

ARTICLE INFO

Keywords:
Species
Biomass
Volume
Land cover
Monitoring
Random forests
Landsat

ABSTRACT

Up-to-date forest inventory information relating the characteristics of managed and natural forests is fundamental to sustainable forest management and required to inform conservation of biodiversity and assess climate change impacts and mitigation opportunities. Strategic forest inventories are difficult to compile over large areas and are often quickly outdated or spatially incomplete as a function of their long production cycle. As a consequence, automated approaches supported by remotely sensed data are increasingly sought to provide exhaustive spatial coverage for a set of core attributes in a timely fashion. The objective of this study was to demonstrate the integration of current remotely-sensed data products and pre-existing jurisdictional inventory data to map four forest attributes of interest (stand age, dominant species, site index, and stem density) for a 55 Mha study region in British Columbia, Canada. First, via image segmentation, spectrally homogenous objects were derived from Landsat surface-reflectance pixel composites. Second, a suite of Landsat-based predictors (e.g., spectral indices, disturbance history, and forest structure) and ancillary variables (e.g., geographic, topographic, and climatic) were derived for these units and used to develop predictive models of target attributes. For the often difficult classification of dominant species, two modelling approaches were compared: (a) a global Random Forests model calibrated with training samples collected over the entire study area, and (b) an ensemble of local models, each calibrated with spatially constrained local samples. Accuracy assessment based upon independent validation samples revealed that the ensemble of local models was more accurate and efficient for species classification, achieving an overall accuracy of 72% for the species which dominate 80% of the forested areas in the province. Results indicated that site index had the highest agreement between predicted and reference (R^2 = 0.74, %RMSE = 23.1%), followed by stand age (R^2 = 0.62, %RMSE = 35.6%), and stem density (R^2 = 0.33, %RMSE = 65.2%). Inventory attributes mapped at the image-derived unit level captured much finer details than traditional polygon-based inventory, yet can be readily reassembled into these larger units for strategic forest planning purposes. Based upon this work, we conclude that in a multi-source forest monitoring program, spatially localized and detailed characterizations enabled by time series of Landsat observations in conjunction with ancillary data can be used to support strategic inventory activities over large areas.

1. Introduction

A key requirement of sustainable forest management is the establishment and maintenance of forest inventories to provide accurate and timely information on the state of the forest that supports a variety of purposes and information needs (White et al., 2016), and most importantly forest planning across a range of scales (Kangas and Maltamo, 2006). Traditionally, inventories have provided relevant information via a suite of attributes including timber volume, mean stand height, and mean tree diameter (Gillis et al., 2005). This information is required to inform strategic planning over large areas and to aid in harvest planning (or to identify locations where information of greater detail is required). Increasingly, forest inventories are being used to relate the provision of other ecosystem goods and services, including habitat characteristics, biotic diversity, and carbon stocks (Laamanen and Kangas, 2011).

In Canada, where extensive forest management practices dominate, forest inventories are often derived from a multi-stage process that involves acquiring aerial photography, using the photos to delineate homogenous units or forest stands, and then interpreting attributes

* Corresponding author.
E-mail address: chen.shang@ubc.ca (C. Shang).

https://doi.org/10.1016/j.jag.2019.101956
Received 11 July 2019; Received in revised form 27 August 2019; Accepted 28 August 2019

from the photography for those delineated stands, often with the aid of stereo vision (Leckie and Gillis, 1995; Gillis and Leckie, 1996). Field plots are then commonly used to adjust regional estimates (Leckie and Gillis, 1995). Forest inventories as a mapped outcome are polygonal in nature (often with a minimum mappable unit of 2 ha), with homogenous stands delineated and attributed to the desired level of detail on the relevant structural, compositional, and functional attributes required by the inventory (Eid et al., 2004). At the most basic, these strategic-level forest inventories are produced to provide forest managers with information to support decisions around timber allocations and harvest planning related to current and projected wood supply (Gillis et al., 2005). As specified, forest inventory are produced on a cycle (e.g., renewed on a decadal basis), with time required for the end-to-end inventory process to be implemented. As a result, inventories are composed of information acquired from different dates and focused preferentially on the managed portions of a jurisdictions' forested land-base. Over time, inventories also use some level of projection to populate polygons that were not represented by new aerial surveys or are not subject to forest management practices (e.g., parks and protected areas). The result is that a given forest inventory typically does not represent the forested land-base uniformly in terms of space, time, or attribution.

Due to the capability of airborne laser scanning (ALS) to provide a detailed three-dimensional view of forest structure (Lim et al., 2003), the technology and related analysis approaches have transformed the derivation of forest inventory in many jurisdictions globally (Reutebuch et al., 2005; Asner et al., 2012; White et al., 2016). Attributes such as stand volume, biomass, diameter, and basal area as well as information on foliage cover and its vertical distribution have all been shown to be accurate (Popescu et al., 2003; Næsset, 2002), often meeting or exceeding the accuracy requirements associated with operational forest management (Magnussen et al., 2012) with relative root mean square errors (%RMSE) typically lower than 20% (Hyyppa and Hyyppa, 2001; Hilker et al., 2008). However, most of these efforts are implemented on an *ad hoc* basis over priority areas (Bolton et al., 2018; Shang et al., 2019). The enhanced forest inventory information generated from these data is of high operational utility, but results in a non-systematic coverage that does not necessarily relay the information required for regional, strategic, monitoring and decision making. Further, the manual elements of the forest inventory process can result in limitations to the quality and consistency of the attributions made (White et al., 2016). This gave rise to the concept of "lidar-plots", where ALS samples sufficient in number and distribution are used to provide independent calibration and validation data (Wulder et al., 2008a, 2012a). For example, Andersen et al. (2011) utilized ALS data in a two-stage approach to predict biomass across Alaska, and Wilkes et al. (2015) used a similar modelling approach with ALS to predict canopy heights across large forest areas of Victoria, Australia. Using imputation techniques, a two-stage approach to estimating forest attributes can be developed using the ALS estimates of forest attributes at select locations over the landscape (Wulder et al., 2012a).

Combining the wall-to-wall coverage of optical satellite data of a known vintage with ALS samples, either as areas (Bolton et al., 2018) or transects (Wulder et al., 2008a), allows for new opportunities to monitor forests (Wulder et al., 2012a). Advances in both the access to and quality of optical remotely sensed data, in particular the 2008 opening of the Landsat archive (Woodcock et al., 2008; Wulder et al., 2012b), offer new opportunities for strategic forest inventory development. Matasci et al. (2018a) combined ALS plot-derived information with Landsat surface-reflectance pixel composite to produce forest structure estimates for over 650 Mha in Canada using nearest neighbour imputation to estimate both ALS metrics of height (e.g., mean height, standard deviation of height) and cover, as well as area-based modeled inventory estimates of Lorey's height, basal area, stem volume, and biomass. These spatial coverages can then be used to inform both the dynamics and regional trends in forest growth and change. Even though wall-to-wall forest attributes maps derived in this fashion cannot fully replace ground-based forest inventory systems, they could contribute to inferences at much finer scales. A number of forest attributes are required to provide the full complement of variables necessary for strategic-level forest inventories (see attribute listing in Falkowski et al., 2009). Forest structural attributes such as height, volume, and cover are critical (Matasci et al. (2018a, 2018b); however, other attributes such as dominant tree species, stand age, site productivity, and stem density are also important forest inventory information for strategic forest planning, which would allow for more specific decisions to be made.

The goal of this research is to present a methodological framework that combines remotely-sensed data and derived products to update existing forest attribute maps in a spatially exhaustive, temporally consistent fashion, over 55 Mha covering the forested area of British Columbia, Canada. The specific research objectives are (i) to assess the utility of object-based image analysis for delineating forest stands using Landsat surface reflectance pixel composites to enable integration with forest stands that are currently used for inventory purposes in the province; and (ii) to examine how a predictive model for dominant tree species calibrated with locally collected training samples compares to a global model calibrated with training samples across the entire study area, in terms of accuracy and efficiency. Ultimately, the approach demonstrated in this research would enable the generation of a more complete suite of forest attribute estimates at a finer level of spatial detail to support strategic level forest planning.

2. Study area

The study area spans the treed area of British Columbia, Canada, totalling over 55 Mha or approximately 59% of the province (Fig. 1). Dominated by mountain ranges, British Columbia features a highly varied climate. As a result, vegetation distribution is controlled by both latitudinal and longitudinal gradients, making it one of the most biologically diverse provinces in Canada (Mathys et al., 2018). The most common tree species in British Columbia include, by area, lodgepole pine (*Pinus contorta*), subalpine fir (*Abies lasiocarpa*), trembling aspen (*Populus tremuloides*), douglas-fir (*Pseudotsuga menziesii*), mountain hemlock (*Tsuga mertensiana*), western hemlock (*Tsuga heterophylla*), and a variety of spruce (*Picea*). Forest management in the province is of economic importance and in most years forest harvesting occurs over an average of 0.17 Mha annually for the period 1985–2015 (White et al., 2017; Natural Resources Canada, 2018). Although fire suppression is common in managed forests, wildfires still occur and can be highly variable in areas impacted on an annual basis. Single recent annual burned areas of greater than > 1 Mha have been reported which are well over the average area burned of less than 0.05 Mha for 1985–2015 (Crowley et al., 2019; White et al., 2017, Hermosilla et al., 2017). Additionally, forests in British Columbia are also affected by non-stand replacing disturbances, such as an outbreak of mountain pine beetle which resulted in high tree mortality impacting trees for an area ~16 Mha over a decade plus period,[1] noting that differences in severity and overlapping of annual survey outcomes can impact reported areas (Wulder et al., 2009). The diversity, nature, and extent of these disturbances underscore the importance, and need for, more frequent forest inventory updates (Bourgeois et al., 2018).

3. Methods

The methodological framework presented in this paper enables the production of wall-to-wall forest attribute maps at the sub-stand level for the entire province of British Columbia, through a combination of

[1] https://www2.gov.bc.ca/gov/content/industry/forestry/managing-our-forest-resources/forest-health/forest-pests/bark-beetles/mountain-pine-beetle/responding-to-the-1999-2015-outbreak

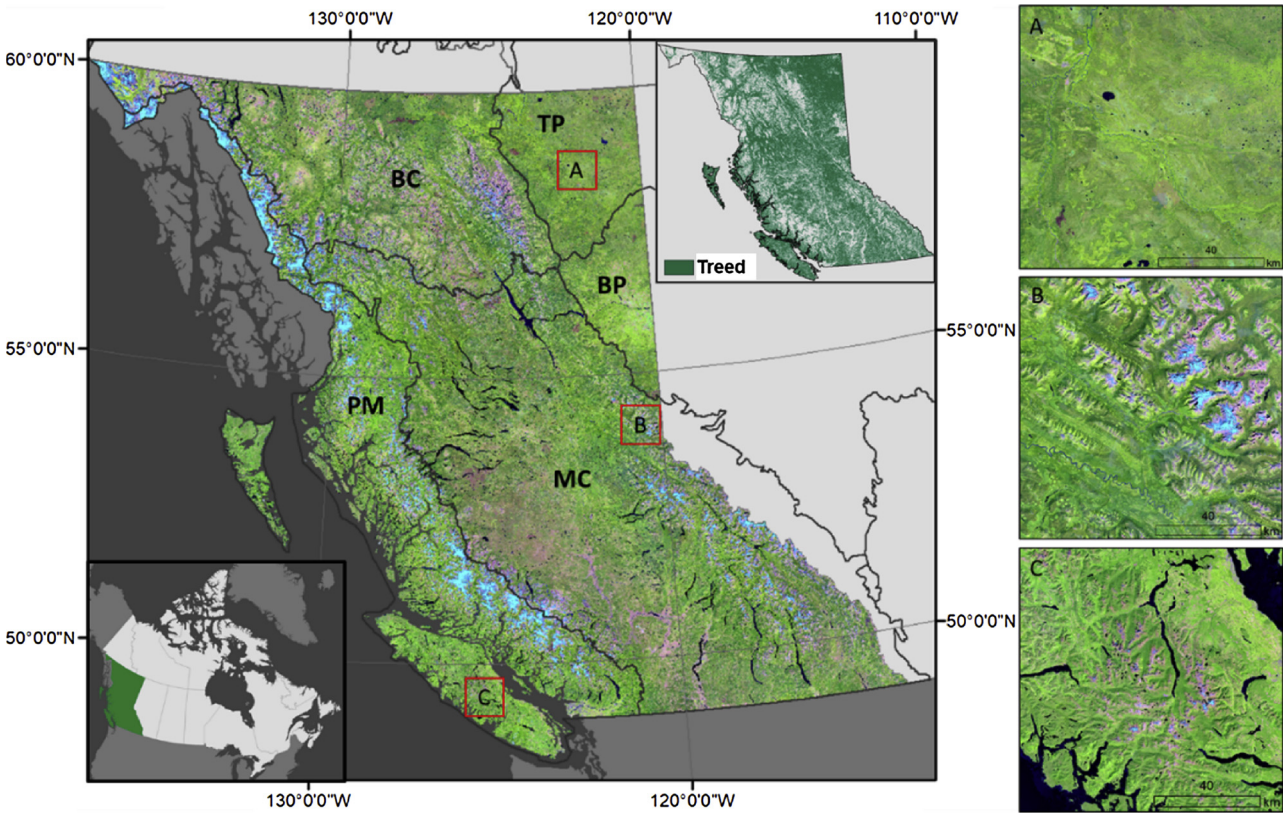

Fig. 1. Study area in British Columbia, Canada, shown with Landsat surface reflectance pixel composite relating 2015 conditions (Red: shortwave infrared band, Green: infrared band, Blue: red band) overlaid with abbreviated ecozones: Pacific Maritime (PM), Boreal Cordillera (BC), Montane Cordillera (MC), Taiga Plains (TP), and Boreal Plains (BP). Three test sites located in northern, interior, and coastal British Columbia are labeled as A, B, and C respectively. The inset shows the satellite land cover derived treed area for British Columbia. (For interpretation of the references to colour in this figure legend, the reader is referred to the web version of this article.)

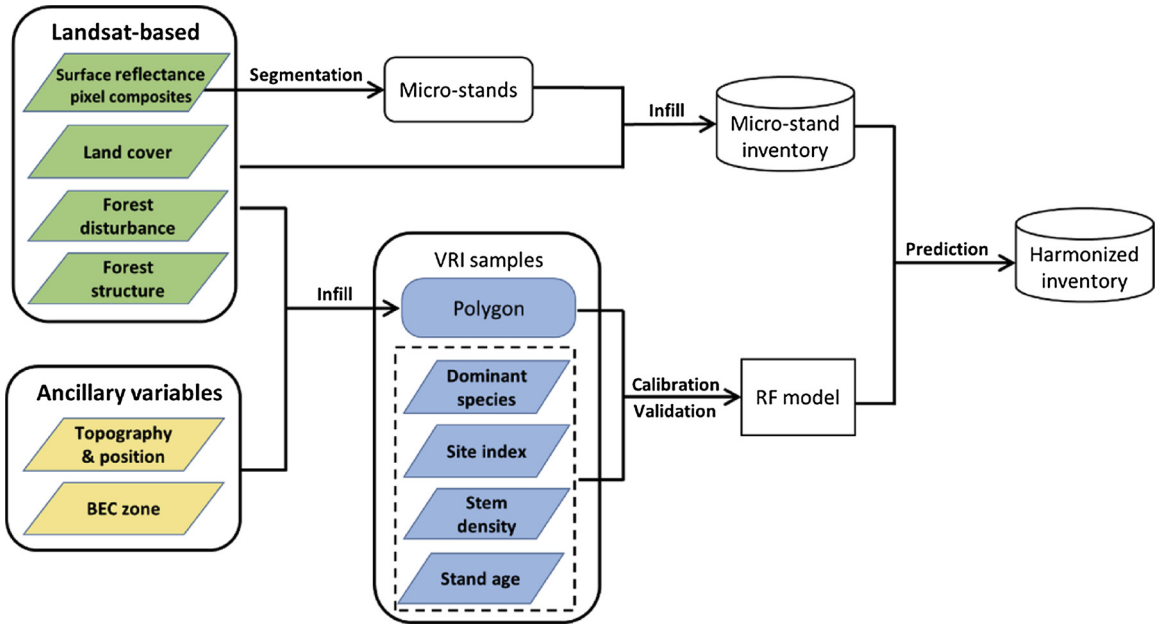

Fig. 2. Overall workflow presenting the suite of predictor variables and steps for stand-level forest attribute modelling and map production.

image segmentation, Landsat-derived spectral, structural, land cover, and disturbance metrics, as well as terrain and environmental data as ancillary variables (Fig. 2). Here we provide an overview of the methodology, with the details discussed in Sections 3.1 through 3.5. First, image segmentation was performed on Landsat surface reflectance pixel composites to derive spectrally-homogeneous micro-stand objects. Best-available pixel composites were generated following the Composite2Change (C2C) approach (White et al., 2014; Hermosilla et al., 2016). Second, the boundaries of these micro-stand objects were used to extract information from Landsat-derived forest structural

Table 1
Predictor variables used to develop the predictive models for our target forest attributes.

Variable group	Variable name	Description	Reference
Landsat surface reflectance composites	TCB	Tasseled Cap Brightness	Hermosilla et al. (2016)
	TCG	Tasseled Cap Greenness	
	TCW	Tasseled Cap Wetness	
Land cover	land cover	Land cover	Hermosilla et al. (2018)
Forest disturbance	disturbance type	Type of disturbance	Hermosilla et al. (2015b)
	year since disturbance	Year since disturbance	
	change persistence	Persistence of change	
Topography	elevation	Elevation	GDEM V2
	TWI	Topographic wetness index	
	TSRI	Topographic solar radiation index	
	slope	Slope	
Geographic location	latitude	Latitude	NA
	longitude	Longitude	
BEC classification	biogeoclimatic zone	Biogeoclimatic ecosystem classification	Pojar et al. (1987)
Forest structure	basal area	Basal area	Matasci et al. (2018a, 2018b)
	elevation cv	Coefficient of variation of vegetation height	
	elevation mean	Average vegetation height	
	elevation p95	95^{th} percentile of vegetation height	
	elevation stddev	Standard deviation of vegetation height	
	volume	Gross stem volume	
	lorey's height	Lorey's height	
	cover 2m	Percentage of first returns above 2m	
	cover mean	Percentage of first returns above mean height	
	biomass	Total above ground biomass	

layers (Matasci et al., 2018a), transforming them from 30-m pixel-based to micro-stand level inventory data. Third, a selection of Landsat-derived products, including surface reflectance pixel composites (Hermosilla et al., 2015a), land cover (Hermosilla et al., 2018), forest disturbance information (Hermosilla et al., 2015b), and forest structural layers (Matasci et al., 2018a) were used, in conjunction with geographical, topographical and climatic ancillary data as predictor variables (Table 1), to model a suite of forest attributes (i.e., dominant species, site index, stem density, and age) available in the vegetation resources inventory (VRI) using Random Forests (Breiman, 2001). Lastly, these predicted forest attributes at the micro-stand level were added to the existing forest structural layers to form a harmonized polygon-based inventory system (Fig. 2). In order to examine the separability of tree species based on our predictor variables, we applied principal components analysis (PCA) to three contrasting sites in British Columbia along a latitudinal and longitudinal gradient (Fig. 1).

3.1. Vegetation resources inventory as response variable

Predictive models of forest attributes over large areas require an extensive network of field data to cover the full range of species and structural variability present across the landscape. To provide a province-wide sample of species and structural conditions, we utilize the current Vegetation Resources Inventory (VRI) data for British Columbia as reference data. As a long-standing provincial inventory program, VRI is an aerial photo interpretation-based inventory program encompassing a range of forest attributes (British Columbia Ministry of Forests, Lands, Natural Resource Operations and Rural Development, 2018). Data acquisition for VRI was carried out following a photo-based, two-stage inventory protocol. First, forest stands were manually delineated as individual polygons and applicable forest attributes were interpreted based on visual characteristics of the aerial photographs. Second, ground sampling was undertaken for calibration and validation purposes. Following delineation and interpretation, a suite of stand-level forest attributes are available, including species composition (up to six species recorded for each stand), height, canopy closure, age, volume, basal area, stem density, and site index (British Columbia Ministry of Forests, Lands, Natural Resource Operations and Rural Development, 2018). Given the relatively large size of the VRI polygons (mean area = 8.5 ha), some of these polygons might not represent homogeneous internal conditions. That is, the forest stand conditions may be consistent for attribution, but there may also be anthropogenic (e.g., road edges, landings) or other natural features (e.g., streams, rock outcrops). Considering this, median values of our predictor variables were extracted for each polygon to reduce the influence of outliers on model development. Additionally, to remove possible edge effects, pixels located along the boundaries between VRI polygons were not considered for computation of median values. Herein, we focused on four attributes from the VRI to expand our suite of forest attributes: stand age, site index, stem density, and dominant species. The definitions and range of values for these attributes are provided in Table 2. It is worth noting that the extreme values for some of the forest attributes are unrealistic, such as a max site index of 90 m and stem density of 21,792 trees/ha. This relates to the subjectivity of the photo interpretation process, where estimates are subject to human errors, which calls for data screening protocols prior to model development and validation.

3.2. Predictor variables

3.2.1. Landsat image composites, forest change and land cover information

To characterize various forest attributes across British Columbia for the target year of 2015, we used Landsat-based surface reflectance composites and forest disturbance information derived following the Composite2Change (C2C) approach (Hermosilla et al., 2016) as well as land cover map computed with Landsat time series (Hermosilla et al., 2018). In summary, a best-available-pixel compositing technique was used to avail upon the entirety of free and open Landsat archive (White and Wulder, 2014; Wulder et al., 2012b) to produce cloud-free, radiometrically consistent composites (Hermosilla et al., 2016, 2017). While the mapping year for this study is 2015, composites, change, and land cover all are informed by time series analysis. The period of analysis aligns with the introduction of 30-m spatial resolution imagery from Landsat-5 in 1984. We acknowledge that 30-m data is theoretically available since 1982 with Landsat-4, but that the data yield was too limited to meet the required density of data coverage (Wulder et al., 2016). From the work in Hermosilla et al. (2016), the average number of images that meet screening requirements and offer pixels to the annual best-available-pixel composites is ~2500 per year (st dev = 878.9). These annual best-available-pixel composites are in turn

Table 2
Descriptions and summary statistics of target forest attributes modeled in this study.

Attribute	Description	Minimum	Maximum	Average	Standard deviation
Stand age	Average age, weighted by basal area, of dominant, co-dominant, and high intermediate trees for the leading and second species of each tree layer identified. Stand age can be based on an estimate from aerial photographs.	1	940	148	83.5
Site index	Mean height that dominant and co-dominant trees are estimated to attain at 50 years. An estimate of site productivity.	1	90	12.2	5.9
Stem density	The average number of living trees visible to the photo interpreter in the dominant and co-dominant crown positions, expressed as stems per hectare.	1	21792	780.6	833.5
Dominant species	Tree species with the highest percentage in terms of canopy cover within a stand.	A total of 25 tree species present. See Fig. 9 for a complete list.			

used to generate Canada-wide image composites following Hermosilla et al. (2015a, 2016).

The target date for the image compositing was set to August 1 st ± 30 days to be within the growing season for most of Canada's forested ecosystems (White et al., 2014). All the available images with ≤70% cloud cover acquired within this temporal window were downloaded from the USGS Landsat archive for the period between 1984 and 2016 as Level-1 Terrain Corrected (L1T) products. Clouds and associated shadows were detected using Fmask (Zhu and Woodcock, 2012). The Landsat Ecosystem Disturbance Adaptive Processing System (LEDAPS) algorithm was applied to compute surface reflectance (Masek et al., 2006). To generate surface reflectance composites with the highest possible fidelity, a scoring function was implemented to select the optimal source of information for each pixel using the following criteria: sensor type, proximity to the target date, distance to cloud or cloud shadow, and atmospheric opacity (White et al., 2014).

Given the varying data availability at different latitudes and persistent cloud presence over certain areas, data gaps in composites were present, representing 10.7% (st dev = 6.1%) of the study area after image compositing. To fill these gaps, spectral trend analyses using the Normalized Burn Ratio (NBR) (Key and Benson, 2006) were performed on the time series imagery at the pixel level, thereby removing the possible noise in the data and filling the gaps through temporal interpolation (Hermosilla et al., 2015a).

Spectral trend analysis also enabled characterization of changes in terms of magnitude, type of disturbance (e.g., harvesting, fire, and non-stand replacing), and temporal dynamics of disturbance (i.e., change persistence and year since disturbance) (Hermosilla et al., 2015b). From the surface reflectance pixel composites for the target year 2015 we derived Tasseled Cap brightness (TCB), greenness (TCG), and wetness (TCW) (Crist, 1985). Furthermore, a series of land cover maps was generated for the study area using the virtual land cover engine (VLCE) approach, which uses temporal information, such as disturbance history, knowledge of vegetation succession, and logical rules to reduce instances of spurious classification results (Hermosilla et al., 2018). The classification scheme consisted of 12 land cover classes in total, of which four are treed classes, including wetland-treed, coniferous, broadleaf, and mixedwood.

3.2.2. Forest structural data

We obtained wall-to-wall, 30-m pixel, structural information from the Landsat-derived forest structural layers produced by Matasci et al. (2018a, 2018b). These forest structural layers represent six imputed ALS metrics (i.e., elevation mean, elevation standard deviation, elevation coefficient of variation, elevation 95th percentile, canopy cover, and canopy cover above mean height), as well as four inventory attributes that were modeled through the combination of ALS and field plot data in an area-based approach (i.e., Lorey's height, basal area, stem volume, and total biomass). Imputations were undertaken using a k-Nearest Neighbor (k-NN) approach with topographic and Landsat spectral predictors, and a Random Forest-based distance metric. With k = 1, the most similar sample for each prediction unit was identified in the training data pool, thus allowing for indirect imputation of the second group of forest attributes (Matasci et al., 2018b) constrained to the treed classes derived from the land cover map (Hermosilla et al., 2018).

3.2.3. Geographical and topographic data

Geographic coordinates (i.e., latitude and longitude) were first derived for the centroid of each Landsat pixel and used as predictors to capture the geographic influences on forest characteristics in a format consistent with our other Landsat-based predictors. Then, a suite of topographic variables were derived from the Advanced Spaceborne Thermal Emission and Reflection Radiometer (ASTER) global digital elevation model (GDEM V2). Compared to the initial version of this DEM released in 2009, this second iteration was developed with

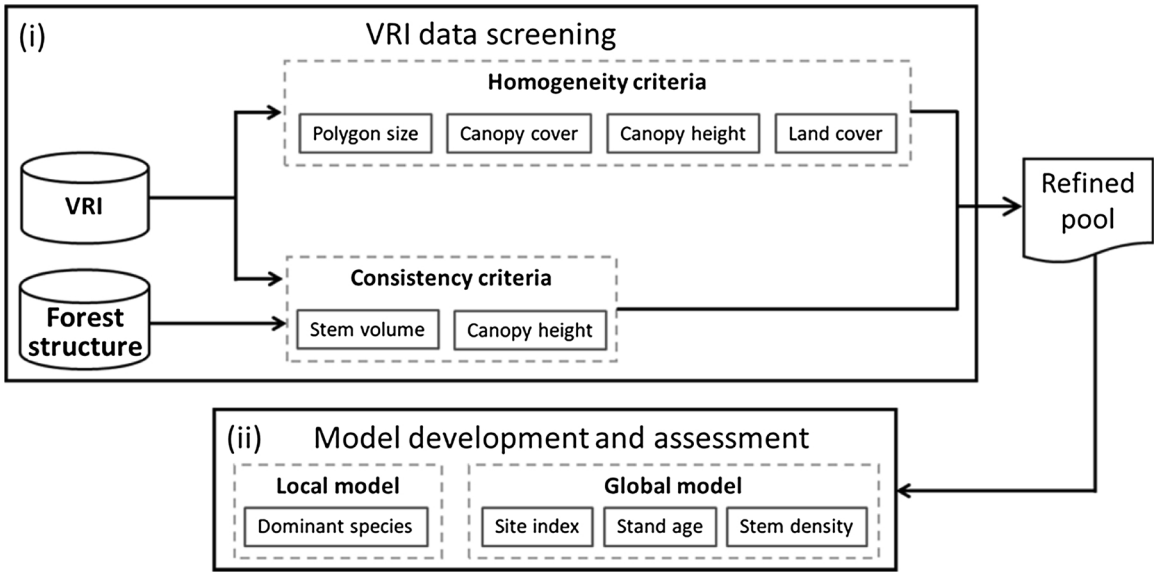

Fig. 3. Workflow diagram consisting of (i) VRI data screening and (ii) model development and assessment.

updated algorithms and an additional 260,000 stereo-pairs from the ASTER sensor onboard the Terra satellite, with 30 m postings (Tachikawa et al., 2011) compatible with Landsat imagery. Derived topographic predictors included elevation, slope, topographic solar radiation index (TSRI) (Roberts and Cooper, 1989), and topographic wetness index (TWI) (Kirkby and Beven, 1979).

3.2.4. Biogeoclimatic ecosystem classification data

Given that forest attributes are influenced by climatic conditions over broad scales (Hamann and Wang, 2006), we incorporated Biogeoclimatic Ecosystem Classification (BEC) into our analysis. Based on vegetation, climate, and soil characteristics, BEC is a well-established classification system that categorizes British Columbia into relatively independent ecosystems (Pojar et al., 1987). With a hierarchical structure, BEC organizes ecosystems at three distinct levels: local, regional, and chronological (MacKinnon et al., 1992). By considering the influence of climate and soil conditions on vegetation, the potential for vegetation can be determined for each site. At the broadest level, BEC zones represent areas under the control of a particular type of macroclimate, characterized by the most dominant tree species. Our study area can be divided into 16 BEC zones, which may contain valuable information for tree species classification (Hamann and Wang, 2006). We used the BEC zones as a categorical predictor variable to characterize the potential associations between climatic and ecological regimes and forest attributes.

3.2.5. Ecozones

We used the ecozones of Canada as a guide to interpret the variations in dominant species classification accuracy at meaningful ecological scales for the province in the results section. In total, there are fifteen terrestrial and five marine ecozones in Canada, each characterized by distinct biotic and abiotic properties. British Columbia covers five terrestrial ecozones, including Pacific Maritime, Boreal Cordillera, Montane Cordillera, Taiga Plains, and Boreal Plains (Ecological Stratification Working Group, 1996).

3.3. Image segmentation for micro-stand establishment

We applied automatic image segmentation over British Columbia-wide Landsat surface reflectance pixel composites to produce polygons of homogenous spectral features that resemble forest stands. Due to its ability to group spatially-adjacent pixels into image segments with relatively high within-segment homogeneity, image segmentation is well-suited for delineating forest stands, as exemplified by Wulder and Seemann (2003); Hay et al. (2005), and Mora et al. (2010). To ensure the homogeneity of our prediction units, the imagery was intentionally over-segmented, producing forest patches at the micro-stand level (Mustonen et al., 2008; Maltamo and Packalen, 2014). A multi-resolution segmentation procedure was implemented in eCognition (Trimble, USA) to segment the Landsat surface-reflectance pixel composites, with scale = 20, shape = 0.1, and compactness = 0.5. Despite the availability of techniques which can automatically determine the optimal parameters for image segmentation (Drăguţ et al., 2014; Gonçalves et al., 2019), these techniques tend to follow specific evaluation criteria not applicable to this study, such as spectral variation in the spatial domain (Woodcock and Strahler, 1987), spatial alignment with reliable reference polygons (Yang et al., 2015), or classification accuracy (Gonçalves et al., 2019). Therefore, segmentation parameters were determined empirically through an iterative process aimed to generate polygons representing relatively homogeneous forest conditions, as per the approach of Wulder et al. (2004a, b). Following image segmentation, each object was characterized with the median values for all the predictor variables, which were used subsequently for generating wall-to-wall forest attribute maps at the micro-stand level.

3.4. Training and validation sample selection from VRI data

As part of our sample selection strategy, we implemented a two-stage data screening procedure to remove records that deviate from pooled data trends and ranges present in the VRI database (Fig. 3). Since high intra-polygon variability represents over generalization in stand delineation (Næsset, 1996), homogeneous VRI polygons were deemed to be of lower uncertainty. To select VRI polygons with homogeneous internal conditions, we implemented the following selection rules: (1) VRI polygon area < 50 ha, (2) number of micro-stands within a polygon < 15, (3) within-polygon height and canopy cover coefficient of variation < 0.5, (4) number of land cover types within a polygon < 2, (5) majority of the polygon covered by treed classes. Sampling ensured that different types of forest stands with varying canopy cover conditions and species composition were eligible for selection. The second phase of sample selection aimed to mask out VRI polygons exhibiting poor correspondence between forest attributes in VRI and the corresponding Landsat-derived forest structural variables (Matasci et al., 2018a, 2018b). Polygons exhibiting significant

Table 3
Descriptive statistics for site index, stem density and stand age in VRI after training pool refinement based on approximately 0.4 million samples.

Attribute	Min	Max	Average	Standard deviation
Stand age (years)	8.0	831.0	148.1	73.2
Site index	2.0	59.9	12.0	4.9
Stem density (stems/ha)	1	5100	742.9	589.1

discrepancy in stand-level estimates were removed from the training pool by developing linear regression models for canopy height and stem volume using all the VRI samples, and samples with the highest residuals (± top 20%) were removed (Fig. 3). Descriptive statistics for the response variables, site index, stem density, and stand age after the training pool refinement are presented in Table 3. The raw VRI data has over 3 million polygons, which was reduced to approximately 0.4 million after these data screening protocols were applied. Compared to the descriptive statistics presented in Table 2, the distributions of the response variables became narrower after the data screening protocols were applied. Considering that the raw VRI data derived from photo interpretation comes with a largely unknown margin of error, this discrepancy highlights the effectiveness of our data screening protocols, aimed to remove VRI polygons that may have unrealistic estimates.

To capture the compositional and structural variability across British Columbia, we divided the study area into a tessellation of 100 × 100 km tiles representing unique geographic zones. Subsequently, training and validation samples were drawn from each zone following a stratified random sampling strategy over all the species present. To characterize the regional particularities of each zone, 8000 training samples were selected from each of the 133 zones in British Columbia, while a total of 12,000 samples were selected for model validation. A subset of the validation samples were used for evaluating species classifications following methods introduced in Section 3.5.5.

3.5. Statistical analysis

3.5.1. Random Forests model

The refined selection of VRI polygons formed the basis of predictive modelling of forest attributes using the Random Forests (RF) technique (Breiman, 2001). As a classic non-parametric modelling technique, the RF model does not make assumptions on data distribution (Breiman, 2001), and is capable of handling both classification and regression tasks (Belgiu and Drăguţ, 2016; Rodriguez-Galiano et al., 2012; Pal, 2005). Specifically, RF regression was performed for continuous variables examined in this study (i.e., stand age, site index, and stem density), and RF classification was applied to discriminate dominant species. RF consists of a number of decision tree models, each trained with a subset of predictors using a bootstrap sample of the original training data. Variable importance scores are determined as the mean decrease in Gini for classification and mean decrease in MSE for regression. For model calibration, we applied the default parameters: number of regression trees (i.e., ntree) was set to 500, the number of predictor variables sampled at each split (i.e., mtry) was set to one third or the square root of the total number of predictors for regression and classification, respectively, and the minimum terminal node size (i.e., nodesize) was set to five.

3.5.2. Dimensionality reduction through variable clustering

Even though RF is relatively robust against collinearity among predictor variables (Penner et al., 2013; Breidenbach et al., 2010; Hudak et al., 2008), the presence of collinearity could impose bias in variable importance derivation and result in suboptimal performance (Chrysafis et al., 2017; Karlson et al., 2015). Therefore, hierarchical variable clustering was employed to reduce the redundancy (i.e., collinearity) among the predictor variables. This clustering technique follows a bottom-up approach, grouping one pair of the most correlated predictors at each iteration until only one cluster remains. Due to the use of synthetic variables to represent each cluster, the ClustOfVAR package in R (Chavent et al., 2011) allows for flexible variable clustering on datasets with a mixture of quantitative and qualitative variables. The optimal number of clusters to retain was computed using the adjusted Rand index (Hubert and Arabie, 1985), which informs on the highest possible intra-cluster homogeneity. As a result, predictor variables falling into the same clusters are highly correlated; therefore, only one predictor was selected to represent each cluster and calibrate the predictive models.

3.5.3. Species separability analysis

To evaluate the spectral and structural separability of the most dominant tree species across different landscapes within the study area, PCA was performed for three sites along a latitudinal gradient prior to the development of the RF models, each with unique species compositions (Fig. 1). The first two principal components (PC) were selected to represent a two-dimensional feature space, where similarity between the most abundant species (top 80%) present in each site was examined.

3.5.4. Local versus global implementation of the RF model

Preliminary analysis of the BEC data indicated that different subregions within British Columbia were occupied by distinct species compositions with varying forest structural characteristics. To examine how selection of training samples influence the predictive power of the RF model, two RF models were developed for species classification: local model and global model. The global model was calibrated with a collection of samples across all the zones introduced in Section 3.4, while the local approach aimed to develop predictive models for each zone independently. Given the large number of VRI polygons available for model calibration, we conducted sensitivity analysis to determine the optimal training sample size for both the local and global model. The effective training sample size for the former was the number of training samples within the individual zones, while that of the latter was carried out by counting the total number of training samples across all the zones in British Columbia. With such a large volume of training data collected over the entire land base of British Columbia, an additional rule was added to the global RF model: for each mapping unit the predicted species is limited to the species compositions of the local zone it resides in, such that species not present in the local region are not predicted by the global model. Based on the premise that the level of association between our predictor variables and the other response variables do not vary as strongly as the case with species, only global models were developed for stand age, stem density, and site index, following similar modelling strategy as the global species classification.

3.5.5. Model assessment

Agreement between VRI data and our model outputs for dominant species, age, site index, and stem density were assessed via independent validation samples. These validation samples were derived in a similar manner as the calibration data, by using the median values within VRI polygons. A sample size of 1200 was selected for validation using a stratified random sampling procedure following Eq. 1 (Cochran, 2007).

$$n = \left(\frac{z}{m}\right)^2 \times p \times (1 - p) \quad (1)$$

where n is the total sample size, z is the percentile associated with the desired confidence interval (1.96 for 95% confidence interval), m represents the margin of error (0.02), and p is the population proportion assumed in this study (0.85).

The allocation of the validation samples followed the recommendation from Czaplewski and Patterson (2003), such that minor classes are over-represented to obtain a comprehensive understanding of the classification system (Eq. 2).

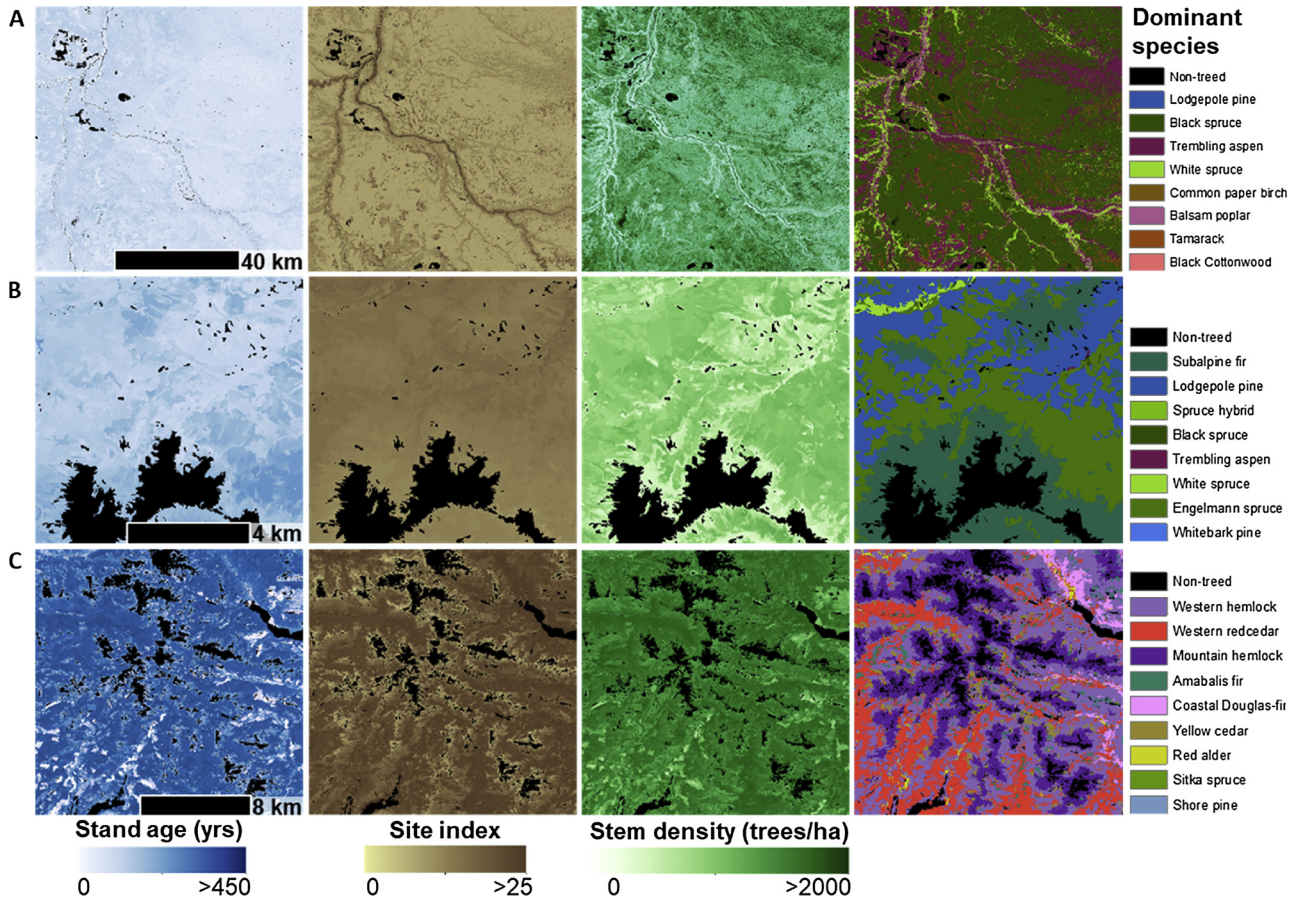

Fig. 4. Predicted stand age, site index, stem density, and dominant species mapped at the micro-stand level for sites A, B, and C at different spatial scales (see Fig. 1 for location of the sites). The non-treed areas consist of non-treed land cover, such as water, snow/ice, exposed land, etc.

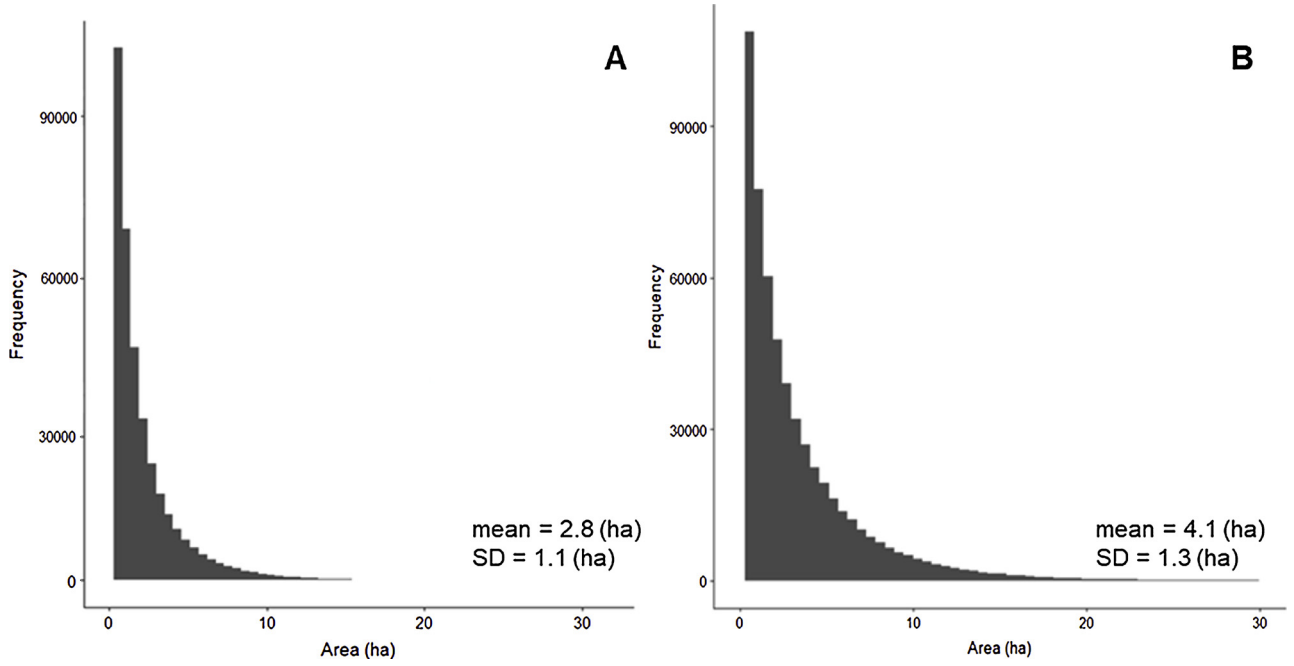

Fig. 5. Size distribution of (A) micro-stand level objects derived from image segmentation, and (B) VRI polygons after the data screening criteria were applied.

$$n_i = p_i \times \frac{n}{2} + \frac{1}{k} \times \frac{n}{2} \quad (2)$$

where n_i is the sample size assigned to class i, p_i is the proportion of area occupied by class i, n represents the overall sample size, and k is the total number of classes.

Confusion matrices were derived for both the global and local species model, and overall, user's, and producer's accuracies were

calculated using a class proportion-adjusted weighting scheme (Olofsson et al., 2014). Performance of the RF regression models for site index, stand age, and stem density was evaluated using coefficient of determination (R^2) and relative root mean squared error (%RMSE).

4. Results

4.1. Forest attribute maps

The predicted stand age, site index, stem density, and dominant species are presented in Fig. 4 for the three select sites in our study area. Overall, there is a moderate agreement between the geographical features exhibited in the four sets of forest attribute maps, especially over large areas. For example, productivity in riparian zones (Fig. 4A) were clearly characterized with relatively high site index, where proximity to water sources also influenced distribution of tree species. At a finer scale (Fig. 4B), the boundaries of the micro-stands become more discernable, showcasing the remarkable amount of spatial details captured in this harmonized polygon-based inventory system. In the medium scale maps presented in Fig. 4C, the important role of topography and landscape position in shaping the development of forests in terms of both species composition and disturbance history is evident.

4.2. Micro-stand characterization

The size distribution of our micro-stand level segmentation and that of the VRI polygons remaining in the training pool after data cleaning (described in Section 3.4) is shown in Fig. 5. In both cases, the majority of the polygons were relatively small in size: approximately 90% of image-derived polygons and 79% of the polygons in the refined VRI pool were respectively below 5 ha in size. However, the distribution of the VRI polygons featured a slightly longer tail, with some polygons exceeding 20 ha. Overall, the size distribution of VRI polygons selected for model development were in alignment with our micro-stand scale objects, which means the training pool selection protocols contributed to controlling the size and intra-polygon homogeneity of VRI.

4.3. Dimensionality reduction

Fig. 6 presents the variable dendrogram obtained from the variable clustering analysis, aimed at reducing the dimensionality of the feature space. Since this clustering technique groups the most similar pair of variables at each iteration, the most correlated variables are grouped together at the bottom of the dendrogram, such as elevation p95 and lorey's height as well as volume and biomass. After the optimal partitioning strategy was determined (depicted in red dotted line), only one predictor was allowed to emerge from the individual clusters of variables, thus reducing the level of collinearity among the predictor variables. Based on the information conveyed, our predictors consist of three major functional groups (Fig. 6). The first one was comprised primarily of geographic and climatic variables (i.e., latitude, longitude, and BEC zone), topographical variables derived from a DEM (i.e., elevation, slope, TSRI, and TWI), and spectral variables derived from Landsat data (i.e., land cover, TCB and TCG), representing environmental conditions. The second functional group was characterized by forest disturbance-related information, such as disturbance type and year of the disturbance. The last cluster consisted of Landsat-derived forest structural variables, such as canopy height, variability of height, cover, and biomass.

4.4. Species separability

In Fig. 7, we report the varying levels of class separability for stand-level dominant species across a latitudinal and longitudinal gradient in our study area. The degree of overlap between the co-occurring species classes varied between 20% and 90% depending on the site. For site C, the distributions of samples for the four most abundant tree species were widespread within the two-dimensional feature space, which implies these species would be difficult to differentiate using parametric models. In contrast, the patterns associated with the most dominant species in site B are easier to discern based on topographical positions and spectral signatures characterized by TCB and TCG. Despite the significant overlaps between species in the feature space for site B and C, it is worth noting the correspondence between species distribution and the predictor variables. For example, the four species in site C exhibited a gradient along PC2, represented by topographical variables, such as elevation and slope, while TCB and TCG also contributed to the differentiation between Spruce hybrid and Engelmann spruce in site B. Therefore, the utility of predictors varied from one site to another for discriminating tree species, relating to the varying driving factors behind a given species distribution.

4.5. Model assessment

4.5.1. Species classification

Fig. 8 depicts the performance of local and global species classifications as a function of training sample size. With small sample size ($n < 500$ per zone), both models performed poorly with an overall

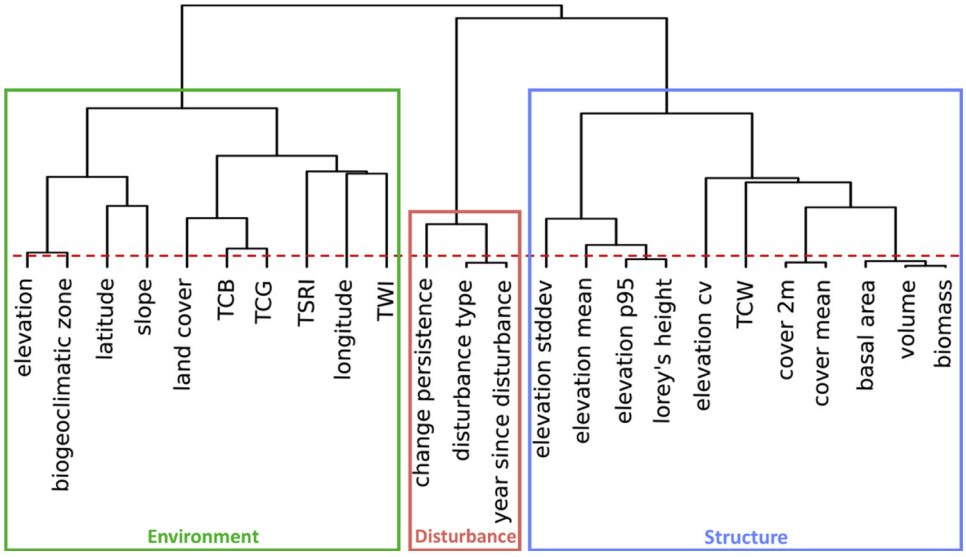

Fig. 6. Variable dendrogram derived from variable clustering analysis. The red dotted line indicates the optimal partition that minimizes the correlation among the remaining predictors yet retains the majority of the information from the input. For interpretation purposes, this variable dendrogram was partitioned into three primary functional groups. (For interpretation of the references to colour in this figure legend, the reader is referred to the web version of this article.)

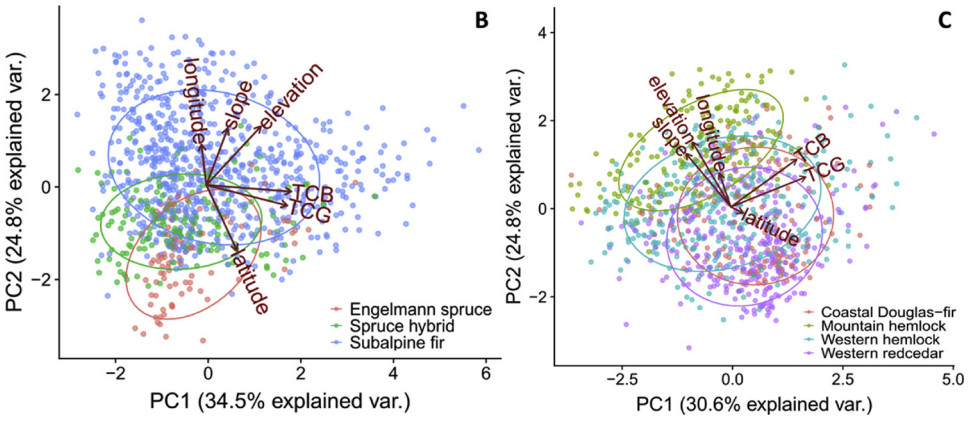

Fig. 7. Distribution of stand-level dominant species in a two-dimensional feature space represented by the first and second principal components derived from PCA based 2000 samples drawn using a stratified random sampling strategy, for test sites B and C. For interpretation purposes, the loadings of only six predictor variables are presented.

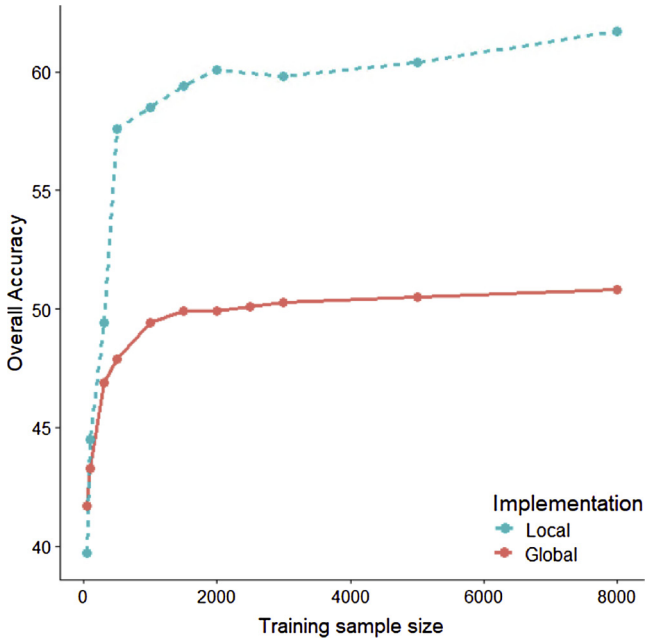

Fig. 8. Sensitivity of the local and global species classification accuracy to training sample size per zone.

accuracy of lower than 50%. As expected, accuracy for both the local and global classification increased as more training samples were selected; however, the rate of increase was markedly different between the two. The local model reached an accuracy of approximately 60% with 2000 training samples per zone, while the global model plateaued at an accuracy of approximately 50% even with much larger sample size across all the zones (i.e., 2500 × 130 zones). In addition to improved classification accuracy, the local species model was more computational efficient than the global model, proving it a more suitable approach for large area mapping.

With 8000 samples per zone, the local species classification reached an overall accuracy of 61.7% globally, and the model generated a species distribution comparable to the reference data over the entire British Columbia (Fig. 9). Even though the final species classification was derived from an ensemble of sub-models calibrated with locally drawn samples, there was a noticeable discrepancy between the observed and predicted species abundance. The rare species were under-predicted, while the more dominant species were over-predicted. Fig. 10 depicts the user's and producer's accuracy for the five ecozones in our study area. Despite the varying accuracies for different species, the user's accuracies were generally higher than producer's accuracy, which means there were generally greater omission than commission errors. Additionally, rare species, on average, had higher user's accuracies than more dominant species, and accordingly lower producer's accuracies, especially in the Montane Cordillera zone. Among the five ecozones, Taiga Plains had the highest overall accuracy at 71.2%, Boreal Cordillera ranked the second with an overall accuracy of 69.1%, followed by Pacific Maritime (68.8%), Boreal Plains (63.4%), and Montane Cordillera (63.1%).

4.5.2. Forest structural attributes estimation

The goodness-of-fit statistics for site index, stand age, and stem density is presented in Fig. 11. Among these three forest attributes, site index had the best fit, with a R^2 of 0.74 and a %RMSE of 23.1%. Relatively good agreement was also found between predicted and reference stand age (R^2 = 0.62, %RMSE = 35.6%). In contrast, stem density was modeled with much lower accuracy (R^2 = 0.33, %RMSE = 65.2%), which was expected given the difficulty in predicting stem density even with active remote sensing instruments (Maltamo et al., 2004; Shang et al., 2019).

4.5.3. Variable importance analysis

In terms of the contribution of different predictor variables to the estimation, environmental predictors encompassing various spectral, geographic and topographic variables were, in most cases, the most important variables for the range of forest attributes examined in this study (Fig. 12), followed by Landsat-derived forest structural variables. The only exception was stem density, which was more closely associated with forest structural information (e.g., TCW). For all the forest attributes, disturbance-related information did not contribute as much to the predictive models, possibly due to the fact that forest disturbances are not reflected in VRI in a timely fashion. Among the individual forest attributes examined, some variations in variable importance were found. For example, climatic information (i.e., BEC zone) was only ranked the 9th most important variable for predicting species, but it made much stronger contributions to modelling site index and stand age.

5. Discussion

The mapping of forest attributes over large areas is challenging due to the extensive and diverse training data required and the related high cost of obtaining a representative sample of field plots over these large geographic extents (Chopping et al., 2008; White et al., 2016). The modelling approach presented herein aims to mitigate these issues by integrating pre-existing large-area forest inventory information and remotely-sensed data in a transparent and systematic modelling framework, which enhances the timeliness of the information and results in greater spatial detail.

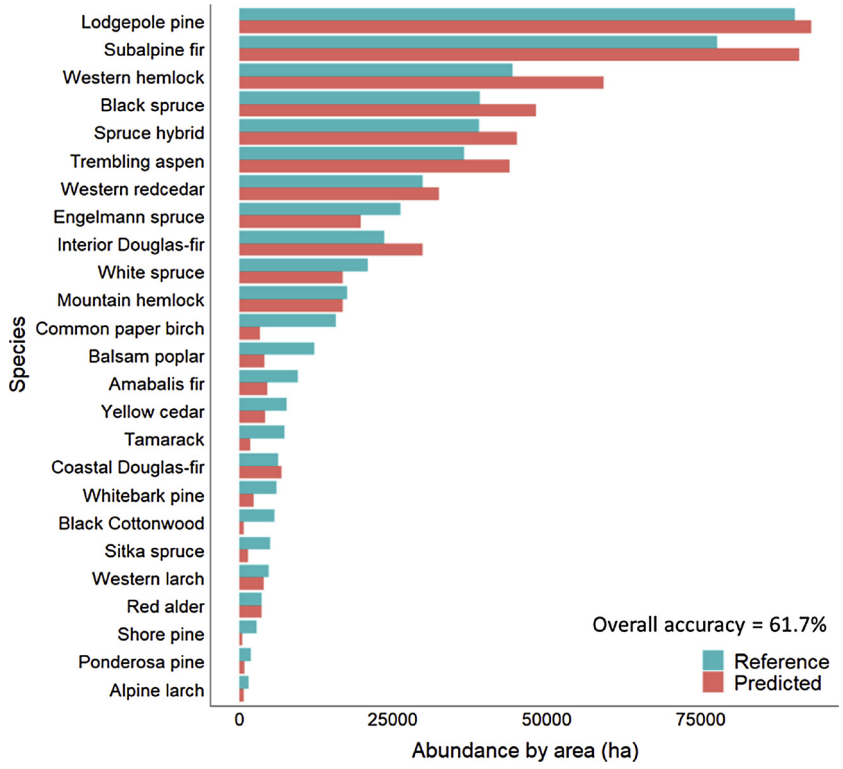

Fig. 9. Overall predicted species abundance compared to reference species abundance weighted by area.

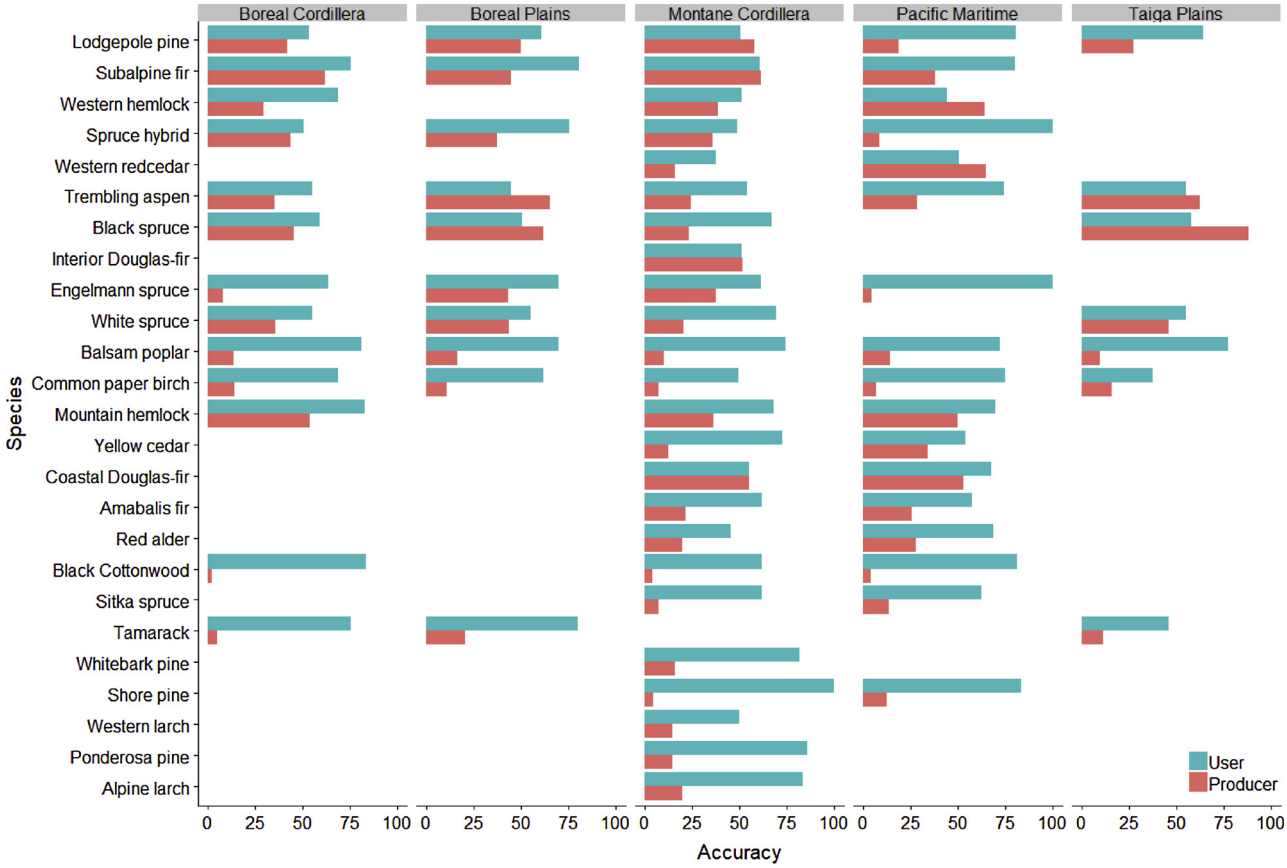

Fig. 10. Producer's and User's accuracy of stand-level dominant species for each of the five ecozones in British Columbia. From top to bottom, the species are arranged in a descending order based on their abundance in British Columbia.

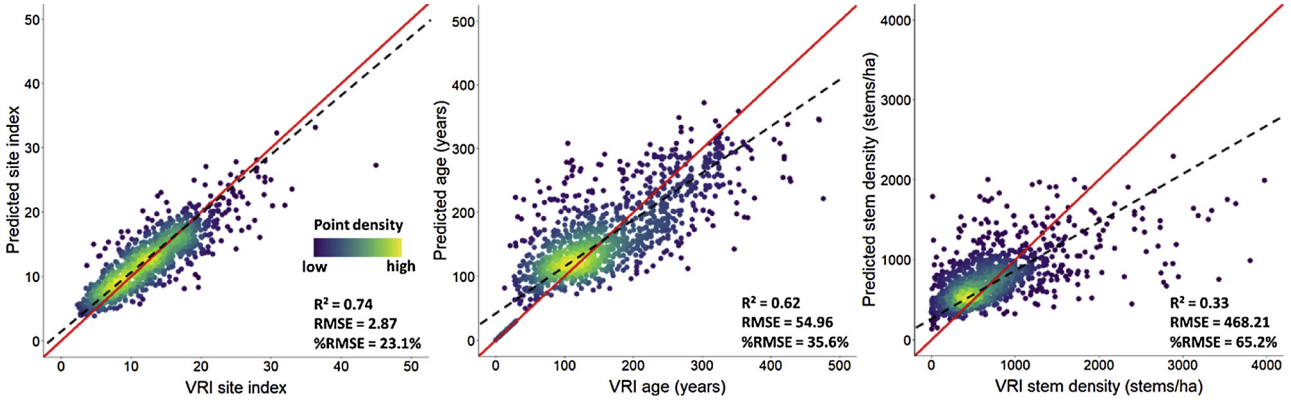

Fig. 11. Predicted versus reference values (VRI) for site index, stand age, and stem density on the 1200 validation samples. Point density is indicated with a purple to yellow color gradient. The 1:1 lines are shown in red, and the regression lines between predicted and reference values are in dashed black. (For interpretation of the references to colour in this figure legend, the reader is referred to the web version of this article.)

5.1. Utility of micro-stand derived through segmentation

Despite the extensive coverage of the VRI data, one inherent issue that arises from aerial photo interpretation is the quality and consistency of forest stand delineation and the estimated attributes across human interpreters. Numerous studies have explored methods to automate the delineation of forest stands from high spatial resolution imagery using object-based image analysis (Hay et al., 2005; Wulder et al., 2008b; Mora et al., 2013). Despite the more coarse spatial resolution of Landsat compared to these high spatial resolution examples, multiple Landsat pixels are containted within forest inventory polygons providing opportunity to derive spectrally homogeneous image objects, described herein as micro-stands. Micro-stands are generated with an aim to reduce the uncertainties associated with larger, more internally heterogeneous, polygons found in VRI (Wulder et al., 2004b). Rather than attempting to directly delineate individual forest stands through image segmentation, a process similar to the super-pixel approach, designed to remove noise and lower the

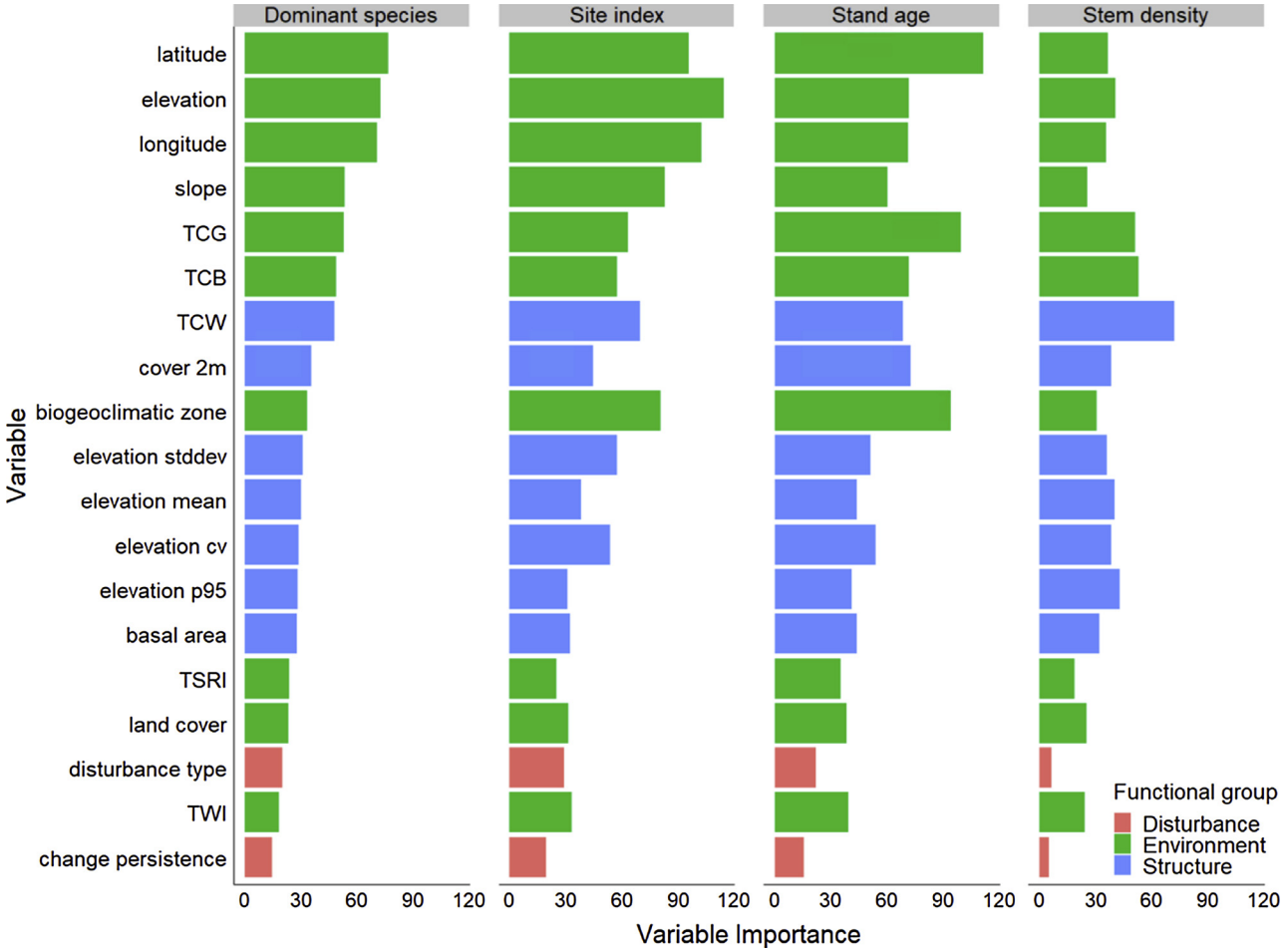

Fig. 12. Variable importance for the four forest attributes modeled in this study. The variables are color coded according to the variable functional groups identified in Fig. 7.

computational hurdle, was implemented (Zhang et al., 2015). Given that these objects are smaller in size compared to the VRI polygons, intra-polygon spectral homogeneity is improved, thereby enabling the development of stronger models. Since forest inventories are traditionally compiled at the stand level, the micro-stands afford additional spatial detail that is normally subsumed in the larger VRI polygon (Figs. 4). The use of smaller micro-stands results in a larger number of data records for the inventory, with implications to data management and analysis. This enhanced information can be carried forward in the inventory as value added, or be removed to avoid any confusion once polygon level attribution is completed. Trade-offs between spatial detail and data management are relevant, but are becoming less of an issue in an age when inventories are fully digital and computational resources are readily available and increasingly cost effective.

A unique challenge pertaining to the integration of remotely-sensed data with pre-existing forest inventory data in a polygon format is the potential differences in scale (Wulder et al., 2006). Considering the small size of the micro-stands obtained from image segmentation, a number of homogeneity criteria were put in place to facilitate the selection of relatively homogeneous VRI polygons as training data. Additionally, data acquisition and interpretation for VRI took place over the time span of several decades (British Columbia Ministry of Forests, Lands, Natural Resource Operations and Rural Development, 2018). Even though several forest attributes were projected to the current date with a growth and yield model, this extensive timespan increased uncertainties of the VRI data. Given that the structural layers derived from Landsat data and ALS plots were generated in a spatially and temporally explicit manner, these layers were used to further refine the selection of VRI polygons for model development, based on the premise that polygons showing good agreement with the predicted structural variables would be more up-to-date and of higher quality. In addition to potential forest disturbance events between acquisition of aerial photographs and our target year 2015, the discrepancy between VRI and Landsat-based forest structural layers could also be a result of inaccurate estimates in photo interpretation and inherent errors associated with the imputed forest structural layers themselves.

These selection criteria contributed to a more robust and reliable pool of training data, which exhibited consistent characteristics with our micro-stands in size distribution (Fig. 5). After the uncertainties in the VRI data were reduced as much as possible, the recurrent observations made by Landsat can be leveraged to update forest inventory information for the entire province with desired update frequency and wall-to-wall coverage. This is particularly cost-effective compared to reacquisition of aerial photographs and interpretation. In addition, the wall-to-wall maps of forest attributes generated from this study would cover areas not previously included in VRI, such as provincial parks. Given the diversity of the training samples used to calibrate our models, these forested areas can be characterized with reportable levels accuracy, thereby satisfying science and policy information needs as well as fulfilling national and international reporting obligations.

5.2. Agreement between predicted forest attributes and VRI

With large volumes of data, a balance between model efficiency and predictive accuracy is of critical importance. The local model of dominant species was developed with spatially constrained training samples, while the global model was calibrated with samples across the entire study area. As revealed in Fig. 7, the level of species separability (i.e., degree of inter-species overlap) varies from one region to another, so do the driving factors behind species distribution. This indicates that species abundance mapping may be highly variable between regions. As expected, the local model outperformed the global model by a large margin both in terms of classification accuracy and computational efficiency. This is likely a result of the inclusion of “impure” samples into the global model. Despite the species that different geographic zones may have in common, the local controls of species distribution were inconsistent, which would result in varying degrees of species separability (Fig. 7). Given that a global model makes predictions in a holistic fashion, differentiation between tree species relies on the same set of rules for the model to perform well. However, training samples collected from multiple geographic areas could increase the heterogeneity of any given class. Even though RF performs a classification by partitioning the training samples into homogeneous pockets in an iterative fashion, the additional intra-class variability introduced from multiple geographic zones likely reduced the accuracy and efficiency of the classification. Zhang and Roy (2017) compared a global implementation of RF land cover classification across North America against a locally adaptive RF variant where part of the training samples are replaced by locally collected samples. At a broader scale, these two approaches made similar predictions; however, the locally adaptive RF model had lower OOB error rates, indicating a stronger agreement between the predicted and reference maps.

Following a similar approach, Thompson et al. (2015) used Landsat BAP pixel composites and topographic variables to model dominant species in Saskatchewan, Canada, with an OOB error rate of approximately 25%. Given the relatively simple species composition for Saskatchewan, only six tree species were examined compared to over 25 species classified in this research, which may in part account for the relatively high accuracy reported in Thompson et al. (2015). As we focus on the top 80% of the species in terms of relative areal coverage in British Columbia, the agreement between VRI and classified species increased to 72%. It must be noted however that species interpretation from aerial photography is also prone to error, which can confound models of species distributions that rely on relatively unique relationships between species and predictor variables. Given that tree species classifications conducted in this study focused on dominant species, the relative proportion (by areal coverage) of species in VRI also influenced the quality of training data, with highly mixed stands being inherently more challenging to classify than pure stands. As we examined the agreement between predicted species and VRI records on an individual zone basis, moderate variations in agreement were found between geographic zones, which may in part be attributed to the local species richness and corresponding driving factors controlling for species distributions (e.g., disturbance history and land form). Additionally, intra-year spectral information has been demonstrated as a means to capture phenology and may be of value in further improving species identification (Dymond et al., 2002; Pasquarella et al., 2018).

The variable importance scores (Fig. 12) corroborated the significant contribution of geographic variables (i.e., latitude and longitude), at both local (species) and broader scales (site index and stand age). This means that the predictive models tend to first select geographic or topographic variables over other predictors to partition the data into relatively homogeneous samples before they are used to refine the predictions. Similar utility of geographic variables has been found for modelling forest structure in existing studies (Zald et al., 2016; Bolton et al., 2018; Matasci et al., 2018b). Stem density, as an exception, did not share the same level of correspondence with geographic/topographic variables. Considering that it also had relatively poor accuracy, the primary driving factors behind stem density are likely absent from our model, such as management interventions, species composition, and stand development stage. Among the three forest structural variables examined in this study, the site index model featured the highest predictive accuracy. Given that site index represents the average height of dominant and co-dominant trees attained at 50 years, it is strongly associated with stand age. However, stand age was predicted with noticeably lower accuracy than site index. This was likely a result of non-linear relationship between stand age and height: the rate of stand height development decreases as it ages (Huang et al., 1992), which might not be captured by Landsat time series data.

6. Conclusion

In this research, we presented an automated methodology to estimate a suite of forest attributes at the stand-level in a transparent and systematic fashion, which allows for a cost-effective means towards updating of jurisdictional strategic forest inventory databases. Following a series of sample selection criteria, a pre-existing polygon-based provincial inventory system was integrated with a selection of Landsat-derived predictor variables to form the basis of our predictive modelling framework. As a part of our modelling strategy, image objects were obtained through multiresolution segmentation, which led to the prediction of forest attributes at the sub-inventory polygon, or micro-stand, level. The comparison between the local and global species classification models revealed that the local model implementation was more suitable for large-area species mapping in terms of predictive accuracy and computational efficiency. Quantitative accuracy assessment demonstrated good agreement between the predicted and reference forest attributes. By leveraging the open Landsat archive and derived data products, the methodology demonstrated in this paper enabled us to map currently estimated (e.g., height, biomass, volume; after Matasci et al., 2018a) and an expanded suite of forest attributes across a large, environmentally and economical important. Integration with current information and processes is buttressed through using pre-existing forest inventory data as the basis for the model training pool and the mapping of outcomes. Given the recurrent nature of satellite observations, this enables more frequent and consistent updating of forest inventory information, thus contributing to more timely and transparent forest monitoring. The approach demonstrated avails upon open access data sets and is portable, suitable for implementation outside of this study area.

Acknowledgements

This research was undertaken as part of the “Earth Observation to Inform Canada’s Climate Change Agenda (EO3C)” project jointly funded by the Canadian Space Agency (CSA), Government Related Initiatives Program (GRIP), and the Canadian Forest Service (CFS) of Natural Resources Canada (NRCan). Support also provided by a NSERC Discovery grant to Coops. This research was enabled in part by capacity provided by WestGrid (www.westgrid.ca) and Compute Canada (www.computecanada.ca). Open access is supported by the Government of Canada.

References

Andersen, H.E., Strunk, J., Temesgen, H., 2011. Using airborne light detection and ranging as a sampling tool for estimating forest biomass resources in the Upper Tanana Valley of Interior Alaska. West. J. Appl. For. 26 (4), 157–164.

Asner, G.P., Mascaro, J., Muller-Landau, H.C., Vieilledent, G., Vaudry, R., Rasamoelina, M., et al., 2012. A universal airborne LiDAR approach for tropical forest carbon mapping. Oecologia 168 (4), 1147–1160.

Belgiu, M., Drăguţ, L., 2016. Random forest in remote sensing: a review of applications and future directions. ISPRS J. Photogramm. Remote. Sens. 114, 24–31.

Bolton, D.K., White, J.C., Wulder, M.A., Coops, N.C., Hermosilla, T., Yuan, X., 2018. Updating stand-level forest inventories using airborne laser scanning and Landsat time series data. Int. J. Appl. Earth Obs. Geoinf. 66, 174–183.

Bourgeois, W., Binkley, C., LeMay, V., Moss, I., Reynolds, N., 2018. British Columbia Forest Inventory Review Panel Summary Report. Prepared for the Office of the Chief Forester Division, British Columbia Ministry of Forests, Lands, Natural Resource Operations and Rural Development.

Breidenbach, J., Næsset, E., Lien, V., Gobakken, T., Solberg, S., 2010. Prediction of species specific forest inventory attributes using a nonparametric semi-individual tree crown approach based on fused airborne laser scanning and multispectral data. Remote Sens. Environ. 114 (4), 911–924.

Breiman, L., 2001. Random forests. Mach. Learn. 45 (1), 5–32.

British Columbia Ministry of Forests, Lands, Natural Resource Operations and Rural Development, 2018. Vegetation Resources Inventory: Photo Interpretation Procedures, Version 3.4. British Columbia Ministry of Forests, Lands, Natural Resource Operations and Rural Development, Forest Analysis and Inventory Branch, British Columbia, Canada.

Chavent, M., Kuentz, V., Liquet, B., Saracco, L., 2011. ClustOfVar: An R Package for the Clustering of Variables. arXiv Preprint arXiv:1112.0295.

Chopping, M., Moisen, G.G., Su, L., Laliberte, A., Rango, A., Martonchik, J.V., Peters, D.P., 2008. Large area mapping of southwestern forest crown cover, canopy height, and biomass using the NASA Multiangle Imaging Spectro-Radiometer. Remote Sens. Environ. 112 (5), 2051–2063.

Chrysafis, I., Mallinis, G., Gitas, I., Tsakiri-Strati, M., 2017. Estimating Mediterranean forest parameters using multi seasonal Landsat 8 OLI imagery and an ensemble learning method. Remote Sens. Environ. 199, 154–166.

Cochran, W.G., 2007. Sampling Techniques. John Wiley & Sons.

Crist, E.P., 1985. A TM tasseled cap equivalent transformation for reflectance factor data. Remote Sens. Environ. 17 (3), 301–306.

Crowley, M.A., Cardille, J.A., White, J.C., Wulder, M.A., 2019. Generating intra-year metrics of wildfire progression using multiple open-access satellite data streams. Remote Sens. Environ (Accepted July 1, 2019, *In press*).

Czaplewski, R.L., Patterson, P.L., 2003. Classification accuracy for stratification with remotely sensed data. For. Sci. 49 (3), 402–408.

Drăguţ, L., Csillik, O., Eisank, C., Tiede, D., 2014. Automated parameterisation for multi-scale image segmentation on multiple layers. ISPRS J. Photogramm. Remote. Sens. 88, 119–127.

Dymond, C.C., Mladenoff, D.J., Radeloff, V.C., 2002. Phenological differences in Tasseled Cap indices improve deciduous forest classification. Remote Sens. Environ. 80 (3), 460–472.

Ecological Stratification Working Group (Canada), Center for Land, Biological Resources Research (Canada), & Canada. State of the Environment Directorate, 1996. A National Ecological Framework for Canada. Centre for Land and Biological Resources Research. State of the Environment Directorate., Hull, Quebec.

Eid, T., Gobakken, T., Næsset, E., 2004. Comparing stand inventories for large areas based on photo-interpretation and laser scanning by means of cost-plus-loss analyses. Scand. J. For. Res. 19 (6), 512–523.

Falkowski, M.J., Wulder, M.A., White, J.C., Gillis, M.D., 2009. Supporting large-area, sample-based forest inventories with very high spatial resolution satellite imagery. Prog. Phys. Geogr. 33 (3), 403–423.

Gillis, M.D., Leckie, D.G., 1996. Forest inventory update in Canada. For. Chron. 72 (2), 138–156.

Gillis, M.D., Omule, A.Y., Brierley, T., 2005. Monitoring Canada’s forests: the national forest inventory. For. Chron. 81 (2), 214–221.

Gonçalves, J., Pôças, I., Marcos, B., Mücher, C.A., Honrado, J.P., 2019. SegOptim—a new R package for optimizing object-based image analyses of high-spatial resolution remotely-sensed data. Int. J. Appl. Earth Obs. Geoinf. 76, 218–230.

Hamann, A., Wang, T., 2006. Potential effects of climate change on ecosystem and tree species distribution in British Columbia. Ecology 87 (11), 2773–2786.

Hay, G.J., Castilla, G., Wulder, M.A., Ruiz, J.R., 2005. An automated object-based approach for the multiscale image segmentation of forest scenes. Int. J. Appl. Earth Obs. Geoinf. 7 (4), 339–359.

Hermosilla, T., Wulder, M.A., White, J.C., Coops, N.C., Hobart, G.W., 2015a. An integrated Landsat time series protocol for change detection and generation of annual gap-free surface reflectance composites. Remote Sens. Environ. 158, 220–234.

Hermosilla, T., Wulder, M.A., White, J.C., Coops, N.C., Hobart, G.W., 2015b. Regional detection, characterization, and attribution of annual forest change from 1984 to 2012 using Landsat-derived time-series metrics. Remote Sens. Environ. 170, 121–132.

Hermosilla, T., Wulder, M.A., White, J.C., Coops, N.C., Hobart, G.W., Campbell, L.B., 2016. Mass data processing of time series Landsat imagery: pixels to data products for forest monitoring. Int. J. Digit. Earth 9 (11), 1035–1054.

Hermosilla, T., Wulder, M.A., White, J.C., Coops, N.C., Hobart, G.W., 2017. Updating Landsat time series of surface-reflectance composites and forest change products with new observations. Int. J. Appl. Earth Obs. Geoinf. 63, 104–111.

Hermosilla, T., Wulder, M.A., White, J.C., Coops, N.C., Hobart, G.W., 2018. Disturbance-informed annual land cover classification maps of Canada’s forested ecosystems for a 29-Year landsat time series. Can. J. Remote. Sens. 44 (1), 67–87.

Hilker, T., Wulder, M.A., Coops, N.C., 2008. Update of forest inventory data with lidar and high spatial resolution satellite imagery. Can. J. Remote. Sens. 34 (1), 5–12.

Huang, S., Titus, S.J., Wiens, D.P., 1992. Comparison of nonlinear height–diameter functions for major Alberta tree species. Can. J. For. Res. 22 (9), 1297–1304.

Hubert, L., Arabie, P., 1985. Comparing partitions. J. Classif. 2 (1), 193–218.

Hudak, A.T., Crookston, N.L., Evans, J.S., Hall, D.E., Falkowski, M.J., 2008. Nearest neighbor imputation of species-level, plot-scale forest structure attributes from LiDAR data. Remote Sens. Environ. 112 (5), 2232–2245.

Hyyppa, H.J., Hyyppa, J.M., 2001. Effects of stand size on the accuracy of remote sensing-based forest inventory. IEEE Trans. Geosci. Remote. Sens. 39 (12), 2613–2621.

Kangas, A., Maltamo, M. (Eds.), 2006. Forest Inventory: Methodology and Applications, vol. 10 Springer Science & Business Media, Dordrecht, Netherlands 362p.

Karlson, M., Ostwald, M., Reese, H., Sanou, J., Tankoano, B., Mattsson, E., 2015. Mapping tree canopy cover and aboveground biomass in Sudano-Sahelian woodlands using Landsat 8 and random forest. Remote Sens. (Basel) 7 (8), 10017–10041.

Key, C.H., Benson, N.C., 2006. Landscape assessment (LA). In: Lutes, Duncan C., Keane, Robert E., Caratti, John F., Key, Carl H., Benson, Nathan C., Sutherland, Steve, Gangi, Larry J. (Eds.), FIREMON: Fire Effects Monitoring and Inventory System. Gen. Tech. Rep. RMRS-GTR-164-CD. US Department of Agriculture, Forest Service, Rocky Mountain Research Station, Fort Collins, CO p. LA-1-55, *164*.

Kirkby, M.J., Beven, K.J., 1979. A physically based, variable contributing area model of basin hydrology. Hydrol. Sci. J. Des Sci. Hydrol. 24 (1), 43–69.

Laamanen, R., Kangas, A., 2011. Large-scale forest owner’s information needs in operational planning of timber harvesting–some practical views in Metsähallitus, Finnish state-owned enterprise. Silva Fenn. 45 (4), 711–727.

Leckie, D.G., Gillis, M.D., 1995. Forest inventory in Canada with emphasis on map production. For. Chron. 71 (1), 74–88.

Lim, K., Treitz, P., Wulder, M., St-Onge, B., Flood, M., 2003. LiDAR remote sensing of forest structure. Prog. Phys. Geogr. 27 (1), 88–106.
MacKinnon, A., Meidinger, D., Klinka, K., 1992. Use of the biogeoclimatic ecosystem classification system in British Columbia. For. Chron. 68 (1), 100–120.
Magnussen, S., Næsset, E., Gobakken, T., Frazer, G., 2012. A fine-scale model for area-based predictions of tree-size-related attributes derived from LiDAR canopy heights. Scand. J. For. Res. 27 (3), 312–322.
Maltamo, M., Packalen, P., 2014. Species-specific management inventory in Finland. Forestry Applications of Airborne Laser Scanning. Springer, Dordrecht, pp. 241–252.
Masek, J.G., Vermote, E.F., Saleous, N.E., Wolfe, R., Hall, F.G., Huemmrich, K.F., et al., 2006. A Landsat surface reflectance dataset for North America, 1990-2000. Ieee Geosci. Remote. Sens. Lett. 3 (1), 68–72.
Matasci, G., Hermosilla, T., Wulder, M.A., White, J.C., Coops, N.C., Hobart, G.W., et al., 2018a. Three decades of forest structural dynamics over Canada's forested ecosystems using Landsat time-series and lidar plots. Remote Sens. Environ. 216, 697–714.
Matasci, G., Hermosilla, T., Wulder, M.A., White, J.C., Coops, N.C., Hobart, G.W., Zald, H.S., 2018b. Large-area mapping of Canadian boreal forest cover, height, biomass and other structural attributes using Landsat composites and lidar plots. Remote Sens. Environ. 209, 90–106.
Mathys, A.S., Coops, N.C., Simard, S.W., Waring, R.H., Aitken, S.N., 2018. Diverging distribution of seedlings and mature trees reflects recent climate change in British Columbia. Ecol. Modell. 384, 145–153.
Mora, B., Wulder, M.A., White, J.C., 2010. Segment-constrained regression tree estimation of forest stand height from very high spatial resolution panchromatic imagery over a boreal environment. Remote Sens. Environ. 114 (11), 2474–2484.
Mora, B., Wulder, M.A., Hobart, G.W., White, J.C., Bater, C.W., Gougeon, F.A., et al., 2013. Forest inventory stand height estimates from very high spatial resolution satellite imagery calibrated with lidar plots. Int. J. Remote Sens. 34 (12), 4406–4424.
Mustonen, J., Packalen, P., Kangas, A., 2008. Automatic segmentation of forest stands using a canopy height model and aerial photography. Scand. J. For. Res. 23 (6), 534–545.
Næsset, E., 1996. Determination of number of stems in coniferous forest stands by means of aerial photo-interpretation. Scand. J. For. Res. 11 (1-4), 76–84.
Næsset, E., 2002. Predicting forest stand characteristics with airborne scanning laser using a practical two-stage procedure and field data. Remote Sens. Environ. 80 (1), 88–99.
Natural Resources Canada, 2018. The State of Canada's Forests: Annual Report 2018. Natural Resources Canada, Canadian Forest Service 84p (Accessed July 10, 2019). https://www.nrcan.gc.ca/our-natural-resources/forests-and-forestry/state-canadas-forests-report/16496.
Olofsson, P., Foody, G.M., Herold, M., Stehman, S.V., Woodcock, C.E., Wulder, M.A., 2014. Good practices for estimating area and assessing accuracy of land change. Remote Sens. Environ. 148, 42–57.
Pal, M., 2005. Random forest classifier for remote sensing classification. Int. J. Remote Sens. 26 (1), 217–222.
Pasquarella, V.J., Holden, C.E., Woodcock, C.E., 2018. Improved mapping of forest type using spectral-temporal Landsat features. Remote Sens. Environ. 210, 193–207.
Penner, M., Pitt, D.G., Woods, M.E., 2013. Parametric vs. Nonparametric LiDAR models for operational forest inventory in boreal Ontario. Can. J. Remote. Sens. 39 (5), 426–443.
Pojar, J., Klinka, K., Meidinger, D.V., 1987. Biogeoclimatic ecosystem classification in British Columbia. For. Ecol. Manage. 22 (1-2), 119–154.
Popescu, S.C., Wynne, R.H., Nelson, R.F., 2003. Measuring individual tree crown diameter with lidar and assessing its influence on estimating forest volume and biomass. Can. J. Remote. Sens. 29 (5), 564–577.
Reutebuch, S.E., Andersen, H.E., McGaughey, R.J., 2005. Light detection and ranging (LIDAR): an emerging tool for multiple resource inventory. J. For. 103 (6), 286–292.
Roberts, D.W., Cooper, S.V., 1989. Concepts and Techniques of Vegetation Mapping. General Technical Report INT-US Department of Agriculture, Forest Service, Intermountain Research Station (USA).
Rodriguez-Galiano, V.F., Ghimire, B., Rogan, J., Chica-Olmo, M., Rigol-Sanchez, J.P., 2012. An assessment of the effectiveness of a random forest classifier for land-cover classification. ISPRS J. Photogramm. Remote. Sens. 67, 93–104.
Shang, C., Treitz, P., Caspersen, J., Jones, T., 2019. Estimation of forest structural and compositional variables using ALS data and multi-seasonal satellite imagery. Int. J. Appl. Earth Obs. Geoinf. 78, 360–371.
Tachikawa, T., Kaku, M., Iwasaki, A., Gesch, D., Oimoen, M., Zhang, Z., et al., 2011. ASTER Global Digital Elevation Model Version 2–Summary of Validation Results August 31, 2011.
Thompson, S.D., Nelson, T.A., White, J.C., Wulder, M.A., 2015. Mapping dominant tree species over large forested areas using Landsat best-available-pixel image composites. Can. J. Remote. Sens. 41 (3), 203–218.
White, J.C., Wulder, M.A., Hobart, G.W., Luther, J.E., Hermosilla, T., Griffiths, P., et al., 2014. Pixel-based image compositing for large-area dense time series applications and science. Can. J. Remote. Sens. 40 (3), 192–212.
White, J.C., Wulder, M.A., 2014. The Landsat observation record of Canada: 1972–2012. Can. J. Remote. Sens. 39 (6), 455–467.
White, J.C., Coops, N.C., Wulder, M.A., Vastaranta, M., Hilker, T., Tompalski, P., 2016. Remote sensing technologies for enhancing forest inventories: a review. Can. J. Remote. Sens. 42 (5), 619–641.
White, J.C., Wulder, M.A., Hermosilla, T., Coops, N.C., Hobart, G.W., 2017. A nationwide annual characterization of 25 years of forest disturbance and recovery for Canada using Landsat time series. Remote Sens. Environ. 194, 303–321.
Wilkes, P., Jones, S., Suarez, L., Mellor, A., Woodgate, W., Soto-Berelov, M., et al., 2015. Mapping forest canopy height across large areas by upscaling ALS estimates with freely available satellite data. Remote Sens. (Basel) 7 (9), 12563–12587.
Woodcock, C.E., Strahler, A.H., 1987. The factor of scale in remote sensing. Remote Sens. Environ. 21 (3), 311–332.
Woodcock, C.E., Allen, R., Anderson, M., Belward, A., Bindschadler, R., Cohen, W., et al., 2008. Free access to Landsat imagery. Science 320 (5879) 1011-1011.
Wulder, M.A., Seemann, D., 2003. Forest inventory height update through the integration of lidar data with segmented Landsat imagery. Can. J. Remote. Sens. 29 (5), 536–543.
Wulder, M.A., Hall, R.J., Coops, N.C., Franklin, S.E., 2004a. High spatial resolution remotely sensed data for ecosystem characterization. BioScience 54 (6), 511–521.
Wulder, M.A., Skakun, R.S., Kurz, W.A., White, J.C., 2004b. Estimating time since forest harvest using segmented Landsat ETM+ imagery. Remote Sens. Environ. 93 (1-2), 179–187.
Wulder, M.A., White, J.C., Luther, J.E., Strickland, G., Remmel, T.K., Mitchell, S.W., 2006. Use of vector polygons for the accuracy assessment of pixel-based land cover maps. Can. J. Remote. Sens. 32 (3), 268–279.
Wulder, M.A., Bater, C.W., Coops, N.C., Hilker, T., White, J.C., 2008a. The role of LiDAR in sustainable forest management. For. Chron. 84 (6), 807–826.
Wulder, M.A., White, J.C., Hay, G.J., Castilla, G., 2008b. Towards automated segmentation of forest inventory polygons on high spatial resolution satellite imagery. For. Chron. 84 (2), 221–230.
Wulder, M.A., White, J.C., Grills, D., Nelson, T., Coops, N.C., Ebata, T., 2009. Aerial overview survey of the mountain pine beetle epidemic in British Columbia: communication of impacts. Journal of Ecosystems and Management 10 (1).
Wulder, M.A., White, J.C., Nelson, R.F., Næsset, E., Ørka, H.O., Coops, N.C., et al., 2012a. Lidar sampling for large-area forest characterization: a review. Remote Sens. Environ. 121, 196–209.
Wulder, M.A., Masek, J.G., Cohen, W.B., Loveland, T.R., Woodcock, C.E., 2012b. Opening the archive: how free data has enabled the science and monitoring promise of Landsat. Remote Sens. Environ. 122, 2–10.
Wulder, M.A., White, J.C., Loveland, T.R., Woodcock, C.E., Belward, A.S., Cohen, W.B., et al., 2016. The global Landsat archive: status, consolidation, and direction. Remote Sens. Environ. 185, 271–283.
Yang, J., He, Y., Weng, Q., 2015. An automated method to parameterize segmentation scale by enhancing intrasegment homogeneity and intersegment heterogeneity. Ieee Geosci. Remote. Sens. Lett. 12 (6), 1282–1286.
Zald, H.S., Wulder, M.A., White, J.C., Hilker, T., Hermosilla, T., Hobart, G.W., Coops, N.C., 2016. Integrating Landsat pixel composites and change metrics with lidar plots to predictively map forest structure and aboveground biomass in Saskatchewan, Canada. Remote Sens. Environ. 176, 188–201.
Zhang, G., Jia, X., Hu, J., 2015. Superpixel-based graphical model for remote sensing image mapping. IEEE Trans. Geosci. Remote. Sens. 53 (11), 5861–5871.
Zhang, H.K., Roy, D.P., 2017. Using the 500 m MODIS land cover product to derive a consistent continental scale 30 m Landsat land cover classification. Remote Sens. Environ. 197, 15–34.
Zhu, Z., Woodcock, C.E., 2012. Object-based cloud and cloud shadow detection in Landsat imagery. Remote Sens. Environ. 118, 83–94.